Supplementary Information

Supplementary information to: Batenburg, S.J., Gale, A.S., Sprovieri, M., Hilgen, F.J., Thibault, N., Boussaha, M., Orue-Etxebarria, X. An astronomical time scale for the Maastrichtian at the Zumaia and Sopelana sections (Basque country, northern Spain).

The position of consecutive 405 kyr minima, using time series analyses of proxy records and lithological observations:

Ma_{405}9: The position of the topmost 405-kyr minimum, the base of cycle Ma_{405}9, can be reliably obtained from correlation to Zumaia from cycle 157 to 185 (Fig. 2, and Batenburg et al., 2012), and is characterized by two limestone-marl alternations in which the lithologies are very similar, indicating a reduced amplitude of the underlying forcing mechanism. Specifically, the limestones of cycles 173 and 174 are not prominent and the marl in between, of cycle 173, is particularly thin and light in colour. Upwards from cycle 171 and downwards from cycle 175, the marls are again darker and thicker. The interval of cycles 172 to175 is characterized by low values of magnetic susceptibility, and a minimum in its 10.7 m filtered component.

Ma_{405}10: Downwards, from cycle 176 to 187, limestones and marls are distinct and cycles are thick, corresponding to a 405-kyr maximum. The interval from cycle 188 to 196 is bounded by marls in which slightly more carbonate rich, but hardly distinguishable, layers occur. These probably represent the very poorly developed limestone-part of a cycle, and have been marked “a” and “b” in the log (Fig. 2). These cycles are likely to have been deposited in the ~ 100-kyr minima of eccentricity within a 405-kyr minimum. In the middle of this interval, the marl of cycle 191 is very thin and light in colour and the limestone of cycle 192 is not prominent. This interval is likely to represent the 405-kyr minimum at the base of cycle Ma_{405}10, which spans 19 cycles and a potential additional cycle marked with “a” and “b”. The minimum interpreted from the lithology coincides with low values, decreased variability, and a minimum in the 10.7 m filtered component of magnetic susceptibility.

Ma_{405}11: Cycles 197 to 205 below consist of distinct limestone-marl alternations. Cycle 206 again has a lighter and more resistant level within the marl, marked with “a” and “b”, likely to represent a 100-kyr minimum close to a 405-kyr minimum. Cycles 206 and 211 have very poorly developed limestones, which are relatively thin and not prominent. Cycles 207 and 212 have the most prominent limestones in this interval and have the lowest values of magnetic susceptibility. This interval is interpreted as the 405-kyr minimum at the base of Ma_{405}11, and coincides with a minimum in the 10.7 m filtered component of magnetic susceptibility.

Ma_{405}12: Cycles 212 to 224 display a very regular alternation of relatively thin limestones and marls in which no bundling can be observed. However, values of magnetic susceptibility are high and variations large, indicative of a 405-kyr maximum of eccentricity. The absence of bundling may be the expression of a longer term minimum in eccentricity which reduces the amplitude of the ~100 kyr cycles. Downwards, cycles 225 to 233 form the uppermost part of a promontory on the beach. The resistance of the beds likely reflects a slightly higher carbonate content. Some bundling can be observed with a relatively dark marl in cycle 227 and in cycles 230 to 233, bounded by intervals with lighter marls. The limestone of cycle 229 is thin and not prominent, and is bounded by light-coloured marls. The limestone of cycle 230 has very low values of magnetic susceptibility. The interval of cycles 225 to 133 coincides with a minimum in the 10.7 m filtered component of magnetic susceptibility and is likely to span the 405-kyr minimum at the base of cycle Ma_{405}12.

$Ma_{405}13$: Cycles 234-244 show distinct limestone-marl alternations with variation in the thickness and colour of the marls. Cycles 234, 238 and 243 in particular have very thin and light-coloured marls, reflecting a bundling of limestone-marl alternations in groups of five. Cycles 245 to 252 form the lowermost part of the promontory on the beach, with relatively little difference among cycles, except in the middle of this interval. The marl of cycle 248 is thin and light, and the bounding limestones of cycles number 248 and 249 are not as prominent as those of neighbouring cycles. The interval coincides with low values of magnetic susceptibility and is interpreted as the 405-kyr minimum of cycle $Ma_{405}13$.

Following page:

Supplementary Table 1: Semi-quantitative distribution range chart of selected calcareous nannofossil taxa in the Zumaia and Sopelana sections. F, few; R, rare, VR, very rare; S, single (see methods for details). Species having biostratigraphical significance are highlighted in pale grey. Dark grey indicates occurrences interpreted as reworked. Modified from Pérez-Rodriguez et al. (2012) for results on the Zumaia section.

sec-tion	cycle	orig. height (m)*	composite (m)	age (Myr)	*Acuturris scotus*	*Broinsonia parca constricta*	*Calculites obscurus*	*Ceratolithoides aculeus*	*Ceratolithoides indiensis*	*Ceratolithoides kamptneri*	*Cribrocorona echinus*	*Lithraphidites quadratus*	*Micula murus*	*Micula prinsii*	*Petrarhabdus vietus*	*Reinhardtites levis*	*Tranolithus orionatus*	*Watznaueria manivitiae s.l.*	*Zeugrhabdotus bicrescenticus*	preservation	bio-events	UC zones
Zumaia (Pérez-Rodríguez et al. 2012)	1	0-0.3	0.00	65.97					R			F	R					F		VP-M		UC20d^P
	2	189.76	0.60	65.98								R	F	R				R		VP-M		
	3	188.5	1.72	66.01					R			F	F					F		VP-M		
	4	188.1	2.08	66.02					R			F	F	R				F		VP-M	Base ***M. prinsii***	
	6	185.9	4.05	66.05								F	F					F		VP-M		UC20c^TP
	7	183.92	5.82	66.09					R			F	R					F		VP-M		
	10	181.15	8.29	66.15						R		F	R					F		VP-M	Base ***C. kamptneri***	
	11	180.3	9.05	66.17								F	R					F		VP-M		UC20b^TP
	17	175.9	13.09	66.29								F	F					F		VP-M	Base ***M. murus***	
	24	170.9	18.03	66.44								F						R		VP-M		UC20a^TP
	37	159.8	28.99	66.72								R						F		VP-M		
	50	148.8	39.86	66.97								F						F		VP-M		
	61	140.8	47.76	67.22					R			R						F		VP-M		
	72	130.54	57.89	67.19				R				R						R		VP-M		
	85b	119.69	68.61	67.47								F						R		VP-M		
	97	110.42	77.77	68.04								R						F		VP-M		
	110	99.8	88.24	68.33	R	R			R									F	R	P-M		
	122	89	98.84	68.56					R									F		VP-M		
	123	87.8	100.02	68.59					R									R		P-M		
	125	86.6	101.20	68.61														F		VP-P		
	128	83.1	104.64	68.68								F						R		VP-M		
	131	79.55	108.12	68.74											R			R		P-M	Top *P. vietus*	
	131	78.8	108.86	68.75								F			R			F		P-M		
	138	74.81	112.78	68.89	?			R	R			R			R			F	R	VP-M		
	142	72.62	114.93	68.97					F			R						R		VP-M		
	143	71.75	115.78	69.00								?						R		VP-P	Base ***L. quadratus***	
	144	70.94	116.58	69.02				R	R						F			F		VP-M		UC19
Sopelana (this study)	157	-	124.08	69.27							S							F		VP	Top *C. echinus*	
	159	-	125.40	69.31														F		VP		
	161	-	127.23	69.35					VR						R	R		F		VP	Top ***R. levis***	UC18
	173	-	135.43	69.61												VR		R		VP		
	175	-	136.67	69.65											S	VR		F		VP	Base *A. maastrichtiana* at Zumaia	
	177	-	138.14	69.69					VR									F		VP-P		
	179	-	139.80	69.73							S							F		VP		
	181	-	141.31	69.77														R		VP		
	183	-	142.94	69.82												S		F		VP-P		
	185	-	144.42	69.86				VR										F		VP-P		
	187	-	145.81	69.90				VR	S		VR							F		VP-P		
	189	-	147.36	69.96				S	S									F		VP		
	191	-	148.78	70.01														F		VP		
	194	-	150.49	70.06				VR	S									F		VP		
	196	-	151.96	70.12														F		VP		
	198	-	153.03	70.17				R	S									F	VR	VP-P	Top *Z. bicrescenticus*	
	201	-	154.88	70.22														R		VP		
	203	-	156.30	70.27				VR	VR									F	VR	VP-P		
	206	-	157.85	70.32			R		R								R	R		VP	Top ***T. orionatus***	UC17
	209	-	159.61	70.40			R	S	S		VR					VR		F	R	VP-P		
	212	-	160.95	70.47			VR		S		VR							F		VP-P		
	214	-	162.31	70.51			S		VR		VR					R		F	VR	VP-P		
	216	-	163.66	70.55							S					S		F	R	VP-P		
	219	-	165.33	70.61			VR		VR									R	S	VP		
	222	-	166.98	70.67												VR		VR		VP		
	225	-	168.52	70.73			R											R		VP		
	227	-	169.82	70.77			R		S							VR		VR	R	VP		
	229	-	171.22	70.81			F	VR								S		R	S	VP-P		
	232	-	172.99	70.87			R				R					VR		F		VP-P		
	234	-	174.39	70.91			R				VR				S	VR		R		VP		
	236	-	176.03	70.96			R				VR					S		F	VR	VP-P		
	238	-	177.47	71.00			F									R		R	VR	VP-P		
	240	-	178.92	71.04	VR		F	VR	R						VR	R	R	F	VR	P		
	243	-	180.50	71.10			F				VR					R		F		VP-P		
	246	-	181.88	71.17			R								VR	VR	S	F	S	VP		
	248	-	183.25	71.21		S	F		S		S					R	S	F	S	VP-P	Top ***B. parca***	16
	251	-	184.84	71.27		R	R	S							S	R		R	VR	VP-P		

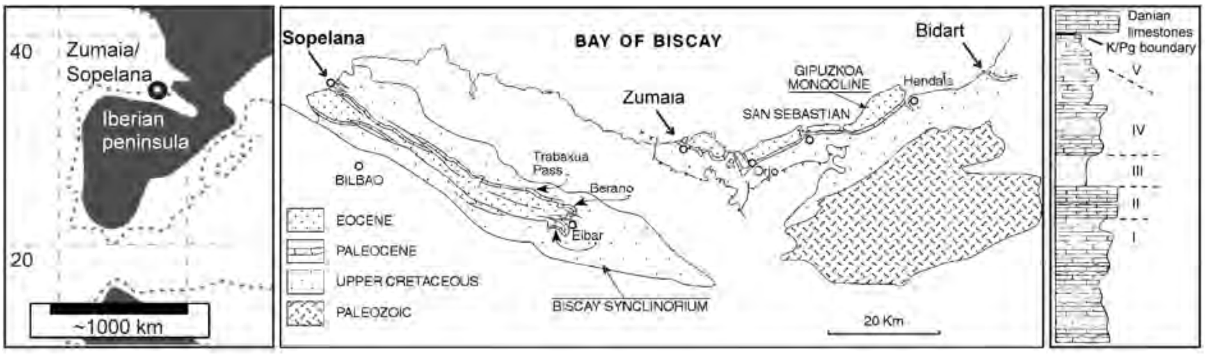

Supplementary Figure 1: Paleogeographic setting (Gómez-Alday et al., 2008), simplified geologic map of the study area from Pujalte et al. (1998) and schematic stratigraphic log from Ward et al. (1991).

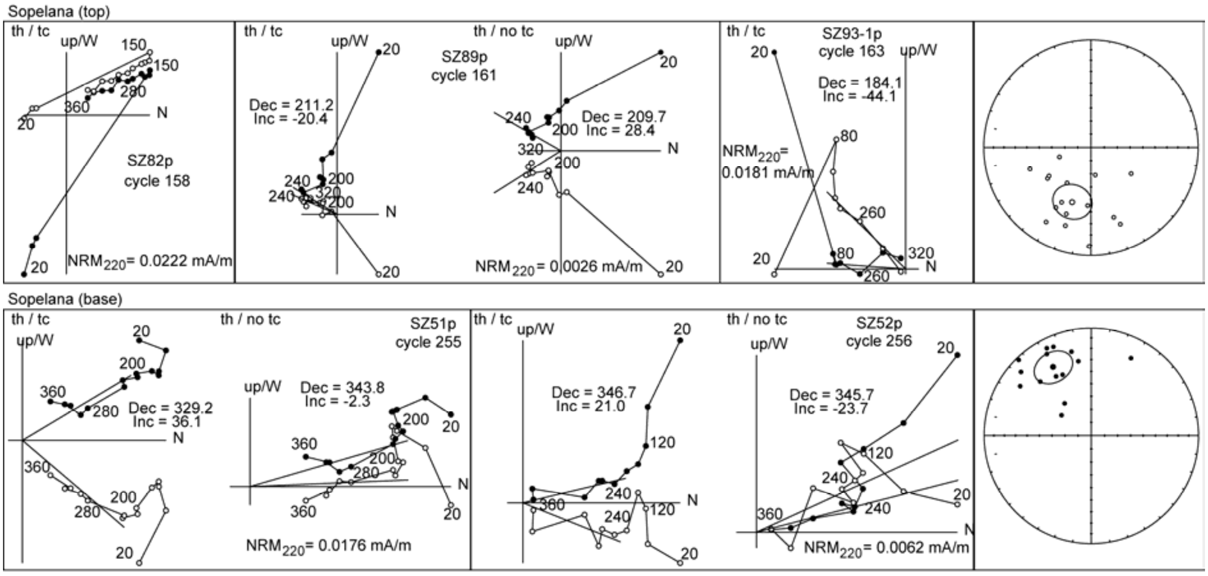

Supplementary Figure 2: Examples of Zijderveld diagrams and equal area projections for the paleomagnetic results of the Sopelana section.

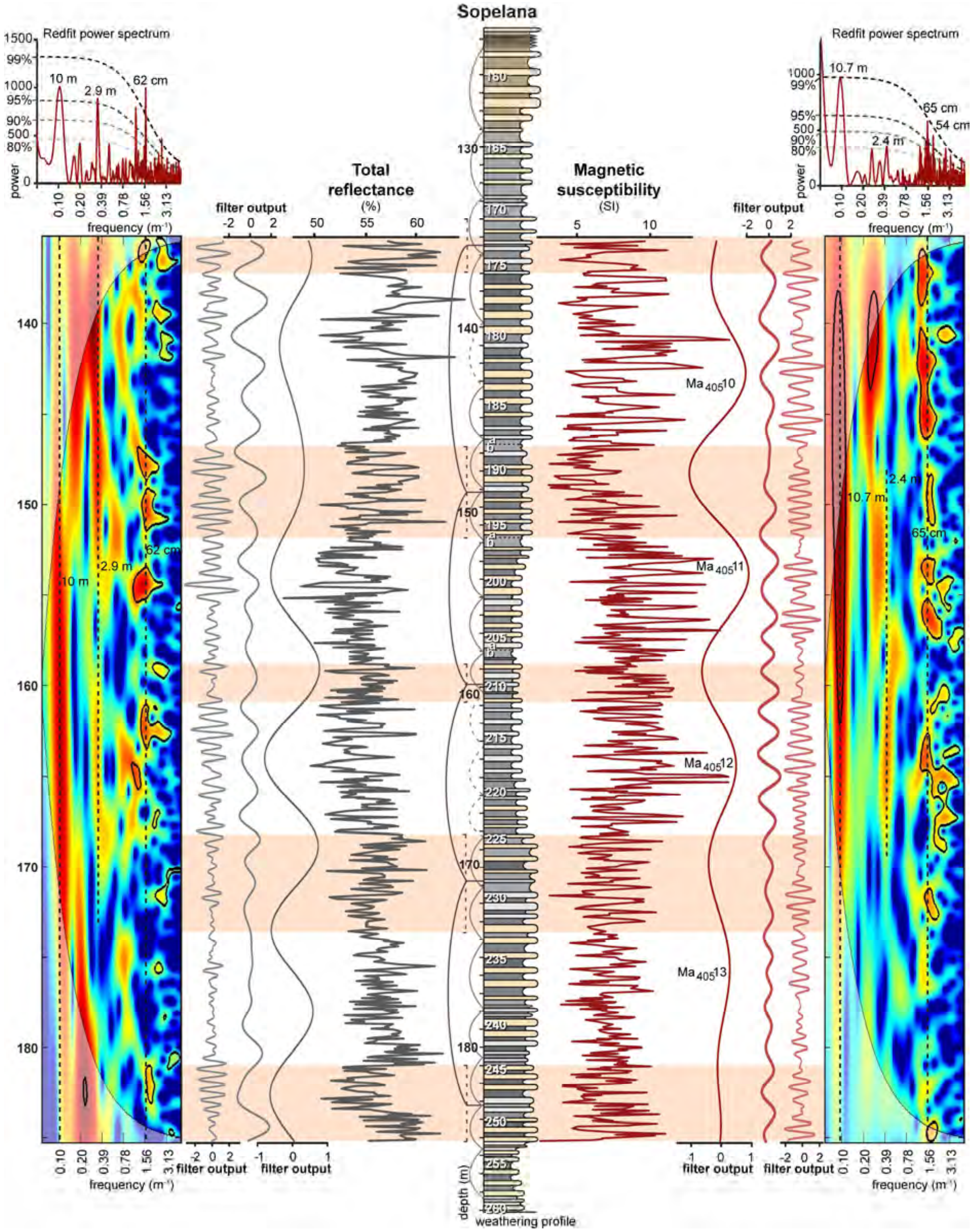

Supplementary Figure 3: Stratigraphic log of the Sopelana section with total reflectance L* on the left and magnetic susceptibility on the right. The data are flanked by their band-pass filters, wavelet analyses and Redfit power spectra. The band-pass filters of reflectance are centred at 10 m (drak grey, bandwidth 7.7-14.3 m), 2.9 m (middle grey, bandwidth 2.0-5.0 m) and 0.62 m (light grey, bandwidth 0.45-1.0 m). The filters for magnetic susceptibility are centred at 10.7 m (dark red, bandwidth 8.1-15.8 m), 2.4 m (red, bandwidth 1.8-3.8 m) and 0.65 m (pink, bandwidth 0.47-1.06 m). The horizontal pink bands indicate the stratigraphic levels that are identified as 405 kyr minima, with the black Ma_{405} numbers indicating the 405 kyr eccentricity cycles following the nomenclature of Husson et al. (2011).

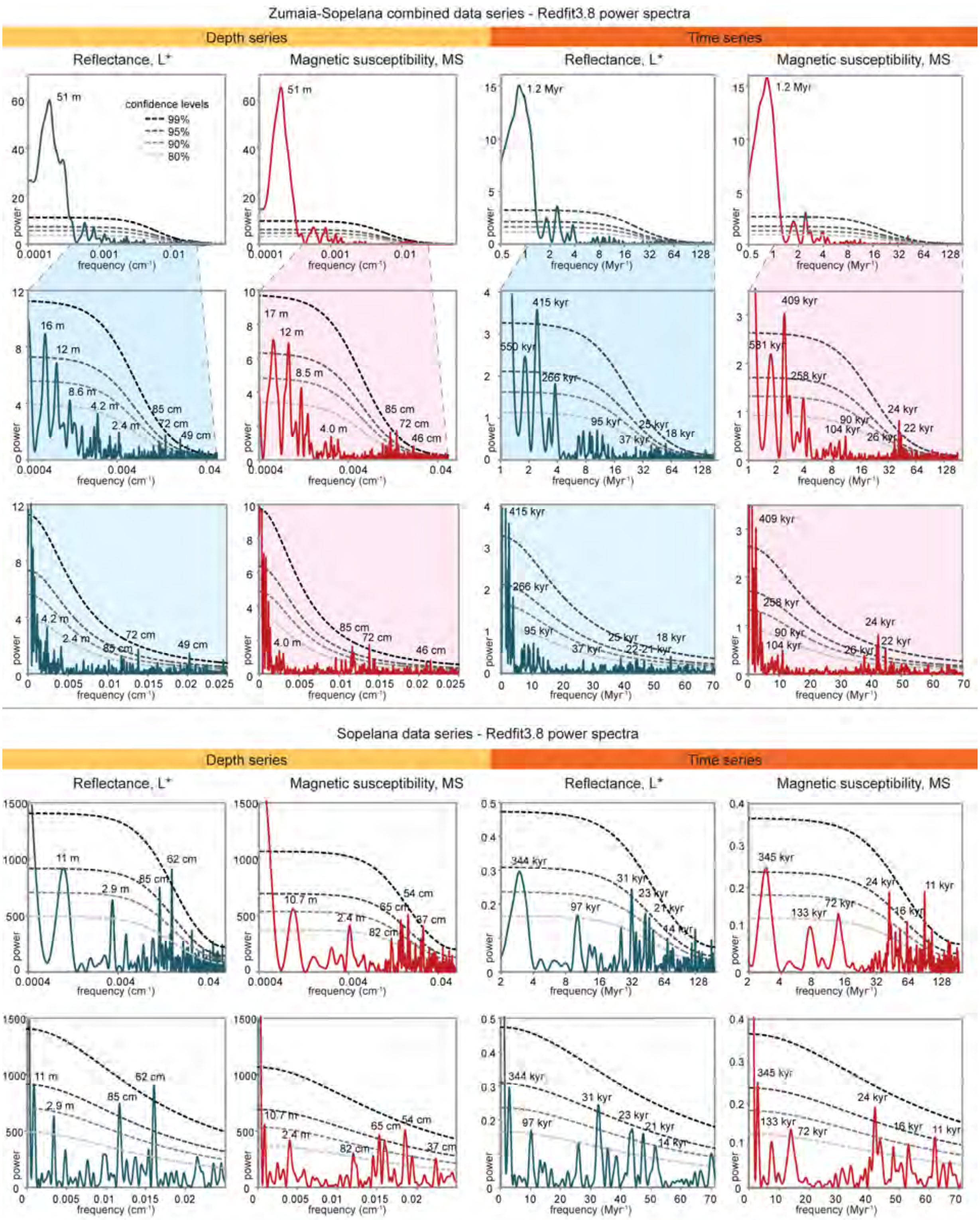

Supplementary Figure 4: Redfit3.8 power spectra of the combined Zumaia-Sopelana data records (top three rows) and the Sopelana data records (bottom three rows) with main periodicities indicated and with 99, 95, 90 and 80% χ^2 confidence levels. Left: power spectra of the Reflectance (L*) records and the Magnetic Susceptibility (MS) records in the depth domain, plotted on logarithmic and linear frequency scales. Right: power spectra of the Reflectance and Magnetic Susceptibility records in the time domain.